

**LNF-05/ 06 (P)**  
**11 April 2005**

**IMPEDANCES OF THE COLD BORE EXPERIMENT, COLDEX,  
INSTALLED IN THE SPS MACHINE**

B. Spataro, D. Alesini  
*LNF-INFN, Frascati, Italy*

M. Migliorati, A. Mostacci, L. Palumbo  
*University of Rome "La Sapienza", and LNF-INFN, Italy*

V. Baglin, B. Jenninger, F. Ruggiero  
*Cern, Geneva, Switzerland*

**Abstract**

This note focuses on the impedances evaluation of the cold bore experiment called COLDEX, and installed in the SPS machine. A comparison between analytical model and numerical results is presented. Tests on power losses are also shown.

PACS.: 41.75; 41:20; 20:27.Bd

*Submitted to  
Nuclear Instruments and Methods in Physics Research, Section A*

## 1 Introduction

In the framework of the electron cloud studies for the Large Hadron Collider (LHC), the cold bore experiment (COLDEX) was installed in the CERN SPS machine in 2002. The experiment is used to simulate a LHC type cryogenic vacuum chamber to study the interaction of such a beam tube with protons beams, particularly electron cloud effects. The 2.2 m long stainless steel cold bore operating below 3 K houses a perforated copper beam screen held at 15 K. At each extremity is placed a 0.3 m long cold/warm transition. To ensure a continuous beam pipe, the cold/warm transition is inserted into the beam screen over 5 mm. The stainless steel cold/warm transition of 0.1 mm thickness limits the thermal conduction to the beam screen.

The global beam screen and cold/warm transition cross section is sketched in Fig. 1. The beam screen is essentially a coaxial line with an inner elliptical cross section and with circular pumping holes of 7 mm diameter located in the horizontal plane. Two rows of 73 holes are spaced by 30 mm. The semi-axes dimensions of the elliptical cross section are 42 mm and 33 mm. The total length of the structure is 2232 mm. The cold/warm transition has the same elliptical shape. Over 20 mm, the extremity located at room temperature adjust the elliptical cross section to a 100 mm circular cross section. During the cool down of the COLDEX beam screen, the beam screen is thermally shrink by 3 mm/m i.e. 6.7 mm. Despite the cold/warm transition is inserted into the beam screen over 5 mm, if all the thermal contraction apply to only one end e.g. during a rapid cool down, one cold/warm transition could be disconnect. To take into account this unlikely event, but to overestimate the heat load in our model, the beam screen and the cold/warm transition are arbitrarily disconnected by 5 mm.

In 2002, the first measurements performed with LHC type protons beams showed large heat load dissipated onto the cold bore and the beam screen [1,2]. When 2 batches of 72 bunches of  $1.15 \times 10^{11}$  protons/bunch were circulating trough COLDEX, heat load from 2 to 12 W were measured onto the beam screen. In order to discriminate all possible source of heat load, a detailed study of the coupling impedance budget for both the beam screen and the cold/warm transition was carried out.

Because of the absence of an axial symmetry of the above components, a numerical approach to the problem based on the use of three-dimensional computer codes has been adopted.

To optimize the accuracy of the results and to minimize the CPU time requirements, the beam screen and the cold/warm transitions have been treated separately obtaining independent impedance estimations, even though the two sections represent a unique structure from the impedance point view.

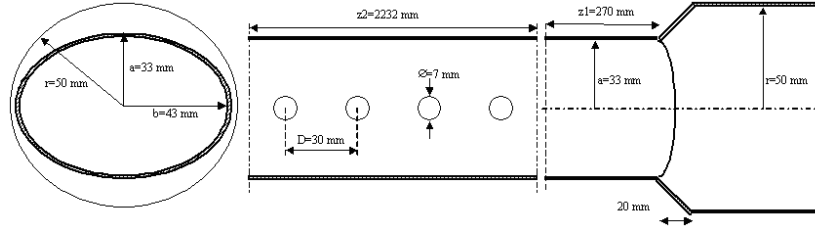


Figure 1: Sketch of half of the COLDEX vacuum chamber. The left and the right side represent the beam screen and the cold/warm section respectively.

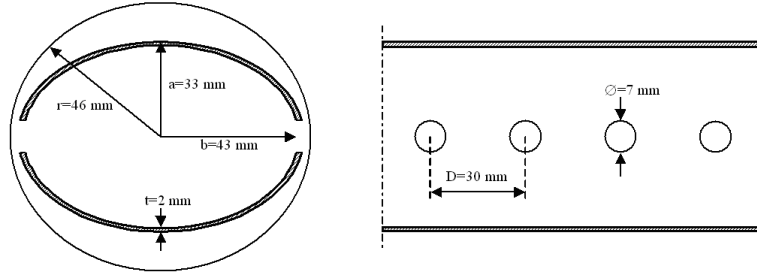


Figure 2: Shape of the beam screen used for Mafia simulations.

In this work the calculations have been made by supposing copper OFHC structures with a conductivity of  $5.91 \cdot 10^7 (\Omega \text{ m})^{-1}$  at room temperature.

The study shows that a circular beam screen with pumping slots would be preferable to reduce the heating. The cold/warm transition studies gave no specific warning, thus no vacuum chamber modification is required. However, the losses due to the impedances are negligible with respect to the measured power onto the beam screen.

The geometries of the beam screen and the cold/warm transition used in MAFIA [3] simulations are reported in Figs. 2 and 3, respectively. Because of the symmetry we have simulated only half structure.

## 2 Uniformly spaced holes

The coupling impedance of a circular coaxial beam pipe with  $N$  pumping holes has been studied extensively by means of the modified Bethe theory; the most important approximations and the main results are reported in [4,5]. Being  $b$  ( $d$ ) the inner (outer) radius of the coaxial beam pipe and  $\alpha_e$  ( $\alpha_m$ ) the electric (magnetic) polarizability of the equally

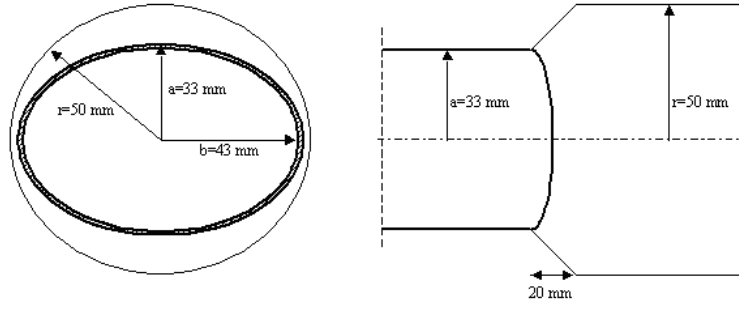


Figure 3: Shape of the cold/warm transition used for Mafia simulations.

spaced pumping holes, the coupling impedance reads

$$Z_{RE}(\omega) = Z_0 \frac{\omega^2 (\alpha_m^2 + \alpha_e^2)}{16\pi^3 b^4 \ln(d/b) c^2} \left[ N + \frac{(\alpha_m + \alpha_e)^2}{\alpha_m^2 + \alpha_e^2} \sum_{h=1}^N \sum_{k=1}^{h-1} e^{\alpha(k-h)D} + \frac{(\alpha_m - \alpha_e)^2}{\alpha_m^2 + \alpha_e^2} \sum_{h=1}^{N-1} (N-h) e^{-\alpha h D} \cos\left(2h \frac{\omega}{c} D\right) \right], \quad (1)$$

$$Z_{IM}(\omega) = Z_0 \frac{\omega (\alpha_m + \alpha_e)}{4\pi^2 b^2 c} N \left[ 1 - \frac{1}{N} \frac{\omega}{4\pi b^2 \ln(d/b) c} \frac{(\alpha_m - \alpha_e)^2}{\alpha_m + \alpha_e} \sum_{h=1}^{N-1} (N-h) e^{-\alpha h D} \sin\left(2h \frac{\omega}{c} D\right) \right], \quad (2)$$

where  $D$  is the hole spacing and  $c$  is the speed of light. The attenuation constant  $\alpha$  accounts of any dissipation in the field propagation; in the case of ohmic losses at room temperature  $\alpha$  depends on the  $\sqrt{\omega}$ . In practical cases, the ohmic dissipation is very small (the beam pipes are built with good conductors) and  $\alpha D \ll 1$ . Both real and imaginary parts depend on the interference among the holes leading to resonance peaks in the impedance at  $\omega_n = n\pi c/D$ .

Far from the resonances, e.g. for  $\omega < \pi c/D$ , the coupling impedance is well approximated by

$$Z_{RE}(\omega) \simeq Z_0 \frac{\omega^2 (\alpha_m + \alpha_e)^2}{16\pi^3 b^4 \ln(d/b) c^2} \left[ \frac{N}{2} + \frac{e^{-\alpha D N} - 1 + \alpha D N}{(\alpha D)^2} \right], \quad (3)$$

$$Z_{IM}(\omega) \simeq Z_0 \frac{\omega (\alpha_m + \alpha_e)}{4\pi^2 b^2 c} N. \quad (4)$$

The real part grows up parabolically with the frequency; for small  $N$ , such as  $\alpha DN \ll 1$ , the exponential term in Eq. (3) can be expanded up to the second order, resulting in an impedance proportional to  $N^2$ . Physically, this is due to the interference effect between the holes which dominates the real part of the impedance. On the contrary, the imaginary part is not affected (at least at a first order) by such an interference and it is mainly due to the holes as they were non interacting. Therefore the imaginary part grows up linearly with  $N$  and with the frequency  $\omega$ , as in Eq. (4).

The loss factor, then, can be expressed as [5]

$$k(\sigma) \simeq \frac{Z_0 \sqrt{\pi} c}{128 \pi^4 b^4 \ln(d/b) \sigma^3} \left[ N^2 (\alpha_m + \alpha_e)^2 + \left( \frac{\sigma}{D} \right)^2 (\alpha_m - \alpha_e)^2 \right]. \quad (5)$$

Again, the dependence on  $N^2$  takes into account interference effect between the holes and it is physically sound. Moreover, if

$$\frac{1}{N^2} \left( \frac{\sigma}{D} \right)^2 \frac{(\alpha_m - \alpha_e)^2}{(\alpha_m + \alpha_e)^2} \ll 1,$$

the loss factor is proportional to  $N^2$ , although it is not  $N^2$  times the loss factor of a single hole (that is proportional to  $\alpha_m^2 + \alpha_e^2$ ). In formulae

$$k(\sigma) \simeq \frac{Z_0 \sqrt{\pi} c}{128 \pi^4 b^4 \ln(d/b) \sigma^3} N^2 (\alpha_m + \alpha_e)^2 \quad (6)$$

if

$$N \gg A \frac{\sigma}{D} \quad A = \frac{(\alpha_m - \alpha_e)}{(\alpha_m + \alpha_e)}.$$

In the case of circular holes in a thin wall, for example,  $A = 3$ .

The energy lost by the bunch in a section of length  $L_d = ND$  is the loss factor times  $Q^2$ , where  $Q$  is the charge of the bunch. Dividing that energy by the time the bunch takes to cover the length of the slotted pipe  $L_d$  (i.e.  $L_d/c$  for relativistic bunches) yields the power flowing in the coaxial and takes into account the effect of a single bunch traveling in the inner pipe. If we assume that the total power is the sum of the power due to each of the  $n_b$  bunches in a length  $L_d$ , we get the expression:

$$P = n_b \frac{c Q^2 k(\sigma)}{L_d} = \frac{c Q^2 k(\sigma)}{S_b}, \quad (7)$$

where  $S_b$  is the bunch spacing ( $S_b = L_d/n_b$ ). In the limit of no attenuation and using Eq. (6) for the loss factor, the contribution of the uniformly holes to the power is

$$P = \frac{\sqrt{\pi}}{128 \pi^4} \frac{Z_0 Q^2 c^2}{\sigma^3} \frac{(\alpha_m + \alpha_e)^2}{b^4 S_b \ln(d/b)} N^2. \quad (8)$$

### 3 Beam screen numerical simulations

Quantitative results of the energy losses, parasitic resonances, longitudinal and transverse coupling impedance have been obtained by MAFIA simulations in time domain. Even if the code allows the study of relatively complicated 3D structures, to get accurate results long computation time and heavy memory resources are needed.

The simulations are not straightforward and require the choice of adequate mesh sizes. Numerical simulations of the cold transition were performed with fine mesh sizes (of the order of 2 mm) and considering only one half of the structure.

To evaluate the short range wake potential over the bunch length (time domain simulations), a single Gaussian bunch with  $\sigma = 12$  cm has been considered (450 GeV proton beam in the SPS). The long range wake potential has been calculated assuming a smaller bunch length ( $\sigma = 1$  cm) over a distance of 6 m behind the bunch. The impedance of the structure has been estimated by the Fourier transform of this long range wake potential.

Since the structure needs a very large number of mesh points, to get a good accuracy and to better understand the results, we have considered four different cases assuming hole diameters equal to 8 mm:

- 18 holes (half structure) with 2 mm mesh sizes;
- 38 holes (half structure) with 2 mm mesh sizes;
- 73 holes (half structure) with 2 mm mesh sizes;
- 146 holes (half structure) with 4 mm longitudinal and 2 mm transverse mesh sizes.

We have evaluated the power losses as a function of the holes number and as a function of the beam position to find if there is a maximum or minimum of these losses and to investigate if there is an interference effect among the holes.

In order to have a deeper insight of the involved physics, intensive calculations of the loss parameters as a function of the vertical and horizontal coordinates, of the beam positions and of the holes number have been carried out.

#### 3.1 Beam screen with 38 holes (19 holes per row)

The longitudinal and transverse (vertical and horizontal) loss parameters [6] as a function of the vertical and horizontal coordinates are reported in Figs. 4a, 4b, and 4c, considering a bunch length of 12 cm. Fig. 4a shows the longitudinal and transverse loss parameters (normalized to their maximum values) along the vertical coordinate of the symmetry plane. We can observe that the maximum value of the longitudinal loss factor occurs at

the geometric center of the structure as it has to be expected because the distance between the beam and the holes is the smallest one. About the transverse loss factor we note that it is directly proportional to the derivative of the longitudinal one as the Panofsky - Wenzel theorem states for coupling impedances. In Figs. 4b and 4c the longitudinal and transverse loss factors as function of the horizontal coordinate (where the holes are located), are reported. It is very interesting to note that the longitudinal loss factor increases strongly (about two orders of magnitude) by going from the geometric center to the holes region while it is almost linear in the center of the pipe. This effect can cause heating of the transition during the machine operation if the orbit is not well corrected.

The average power  $P$  lost by the beam is:

$$P = K_l I^2 T N_b; \quad (9)$$

with a longitudinal loss parameter calculated at the geometric center  $K_l = 1.56 \cdot 10^4$  V/C, an average current  $I = 0.7$  mA per bunch, a revolution time  $T = 23 \cdot 10^{-6}$  s, and with a number of bunches  $N_b = 288$ , we get a power loss  $P = 0.051$  mW. The gradient of the longitudinal loss factor with respect to the horizontal coordinate and near the center of the pipe is  $\partial K_l / \partial x = 2810$  V/(C mm). As a consequence the power gradient is  $\partial P / \partial x = 9.1$   $\mu$ W/mm.

Concerning the transverse loss factor, close to the geometric center of the pipe, the horizontal one is three times higher than the vertical one. For this reason we present results only for the horizontal displacement of the beam.

In the region where the horizontal loss factor exhibits a linear behavior with the displacement, the following relation can be applied [7]:

$$Im(Z_t) = -2 \frac{\sigma K_t \sqrt{\pi}}{c} \quad (10)$$

giving a transverse impedance of  $Z_t = 25.13$   $\Omega$ /m, with  $\partial K_t / \partial x = 1.77 \cdot 10^{10}$  V/(Cm)

As far as the longitudinal coupling impedance is concerned, we calculated the short range wake potential over the bunch length by assuming  $\sigma = 12$  cm. The normalized wake potential is reported in Fig. 4d. It is clear that the transition is purely inductive at low frequencies. From the simulations we have that the absolute maximum values of the wake potential are  $|W_{max}| = |W_{min}| = W = 1.831 \cdot 10^7$  V/C. By using the theoretical relation [8]:

$$W = \frac{Lc^2}{\sqrt{2\pi e\sigma^2}} \quad (11)$$

we can estimate the inductive longitudinal impedance  $|Z/n| = \omega_0 L = 3.31 \cdot 10^{-6}$   $\Omega$ .

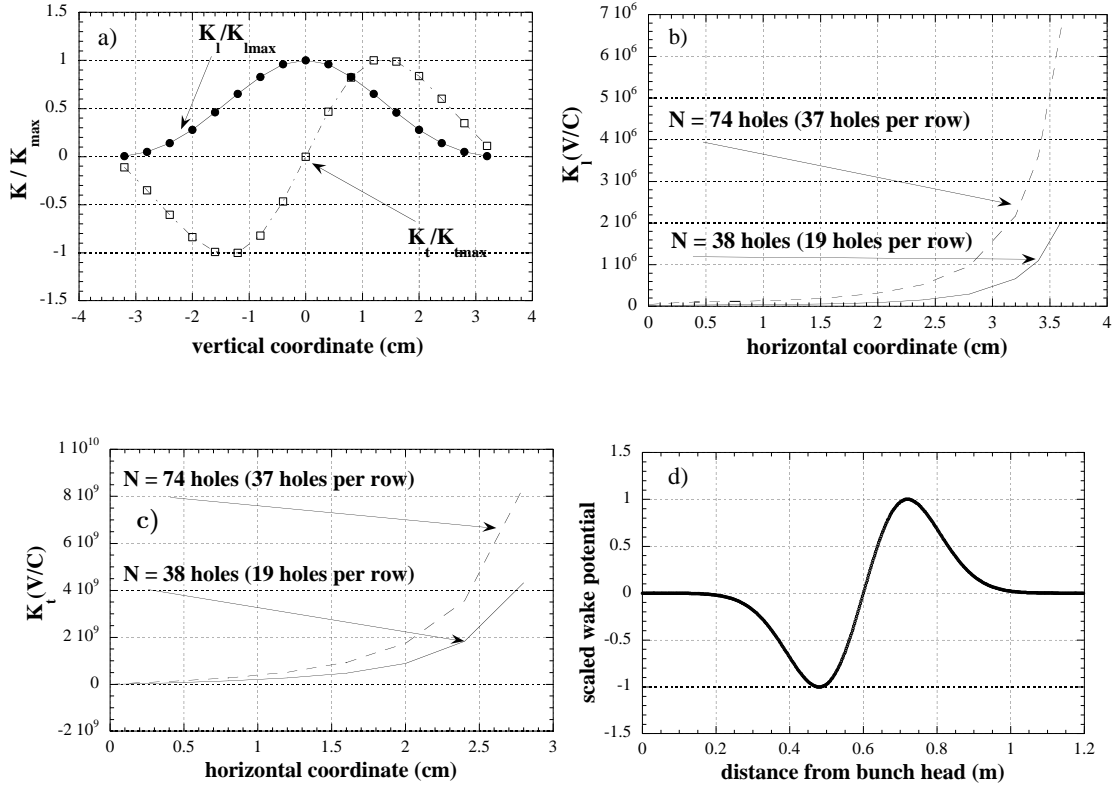


Figure 4: a) Normalized longitudinal and transverse loss parameters along the vertical coordinate of the symmetry plane for  $N = 38$  and  $74$  holes. For  $N = 38$ ,  $K_{lmax} = 1.56 \cdot 10^4$  V/C and  $K_{tmax} = 6.2 \cdot 10^7$  V/C; for  $N = 74$ ,  $K_{lmax} = 5.132 \cdot 10^4$  V/C and  $K_{tmax} = 1.2 \cdot 10^8$  V/C. b) Longitudinal loss parameter versus the horizontal coordinate. c) Transverse loss parameter versus the horizontal coordinate. d) Normalized wake potential versus the distance from bunch head. For  $N = 38$  the maximum value is  $1.8 \cdot 10^7$  V/C and for  $N = 74$  is  $3.6 \cdot 10^7$  V/C.

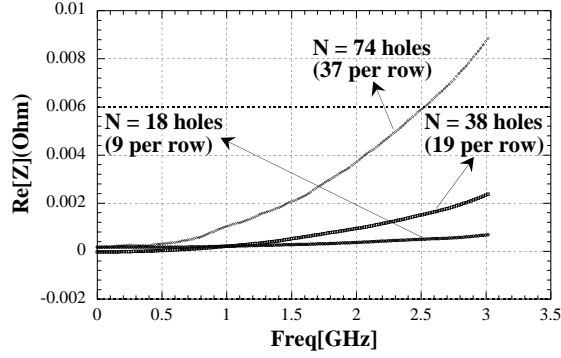


Figure 5: Longitudinal coupling impedance for different values of hole number as a function of frequency.

### 3.2 Beam screen with 74 holes (37 per row)

To investigate the behavior of the longitudinal and transverse loss factors as a function of the holes number, simulations were performed with 74 holes. The corresponding results are still reported in Figs. 4a, 4b, 4c, and 4d.

Figure 4a shows the longitudinal and transverse loss parameters normalized to their maximum values on the vertical symmetry plane. These results reproduce the behavior of the previous case with 38 holes. The calculated longitudinal loss factor in the center of the pipe is  $K_l = 5.132 \cdot 10^4$  V/C and it yields a power losses  $P$  of 0.17 mW. The gradient of  $K_l$  (see Fig. 4b) as a function of the horizontal coordinate is  $\partial K_l / \partial x = 9229$  V/(C mm) and the related the power gradient is  $\partial P / \partial x = 30$   $\mu$ W/mm. The calculated transverse impedance (see Fig. 4c) is  $Z_t = 49$   $\Omega$ /m with  $\partial K_t / \partial x = 3.45 \cdot 10^{10}$  V/(Cm), while the longitudinal impedance is  $|Z/n| = 6.4 \cdot 10^{-6}$   $\Omega$  with  $|W_{max}| = |W_{min}| = 3.565 \cdot 10^7$  V/C.

The coupling impedance at low frequencies is shown in Fig. 5 for 3 different values of the hole number  $N$ . The parabolic behavior is clear from the plots and can be highlighted by a polynomial fit. The result is shown in Table 1 where the correlation coefficient  $R$  states the quality of the fit: it is equal to 1 for an optimal fit.

The ratio  $a_{N_i} / a_{N_j}$  is very close to  $(N_i / N_j)^2$ , as it should be from Eq. (3).

### 3.3 Parasitic resonances

To completely characterize the structure, we have calculated the 6 m long range wake potential considering a Gaussian bunch of  $\sigma = 1$  cm traveling trough the structure 4 mm away from the holes; in fact, such a short distance allows a better measurement of the resonance amplitudes. The Fourier transform of this wake potential gives the impedance

$Re(Z)=a_N f^2 + b_N f + c_N, (N = 18, 38, 74)$			
$a_N$	$b_N$	$c_N$	$R_N$
$6.2 \cdot 10^{-5}$	$-2.4 \cdot 10^{-5}$	$1.66 \cdot 10^{-4}$	0.9992
$2.72 \cdot 10^{-4}$	$-6.53 \cdot 10^{-5}$	$-9.9 \cdot 10^{-6}$	0.9996
$1.03 \cdot 10^{-3}$	$-3.16 \cdot 10^{-4}$	$2.23 \cdot 10^{-4}$	0.9998

Table 1: Parabolic fit of the real coupling impedance for  $N = 18$ ,  $N = 38$ ,  $N = 74$  as a function of frequency  $f$  (expressed in GHz).

of the structure at that beam position. The cut-off frequencies of the vacuum chamber calculated by OSCAR2D [9] are 2.11 GHz for the TE mode polarized with the E-field parallel to the major axis and 2.63 GHz for the other TE mode.

The real and imaginary part of the longitudinal coupling impedance and the normalized wake potential with 38 holes are illustrated in Figs. 6a, 6b, 6c. The real and imaginary part of the transverse coupling impedance and the normalized transverse wake potential are reported in Figs. 7a, 7b, 7c. The results obtained with 74 holes are shown in Figs. 8a, 8b, 8c for the longitudinal case and in Figs. 9a, 9b, 9c for the transverse one. Comparing the results of the pictures related to 38 and 74 holes, one observes that at low frequency (up to  $\sim 4$  GHz) the impedance is purely inductive. At low frequency the imaginary part scales with  $\omega$ , as expected from theory. The real part, as already observed, is proportional to  $\omega^2$  and exhibits resonant peaks. The maximum amplitude of the resonances depends on the proximity of the beam to the slotted wall, but they are always present. In the simulations, their amplitude scales with  $N$ , due to the small number of points used to resolve the resonances.

The plots clearly show some parasitic resonances in the 4 - 12 GHz frequency range very far from the bunch spectrum cut-off. It is worth noticing that the strongest resonance is peaked at about  $f = 9.27$  GHz. This frequency corresponds to a wavelength equal to the holes distance. For an additional confirmation of this parasitic resonance related to the holes distance, we have simulated the case of a 28 mm distance between the holes. As a result, the corresponding frequencies of all the parasitic resonances scale proportionally to the distance between two hole centers.

The impedances follow the same dependence with  $N$  as discussed in the previous section.

In conclusion, since most of the bunch spectrum is very far from these resonances, no effective interference between the holes exists.

For increasing our confidence with the presented analysis, we have simulated a

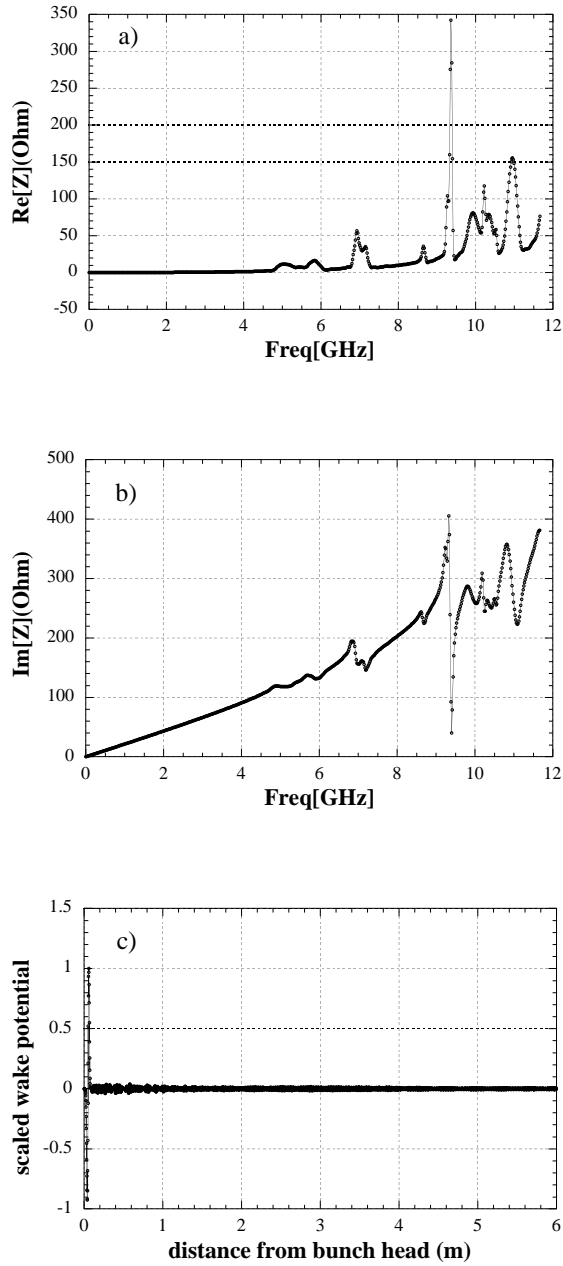


Figure 6: Longitudinal coupling impedance for  $N = 38$ : a) Real part, b) Imaginary part, c) Scaled wake potential.

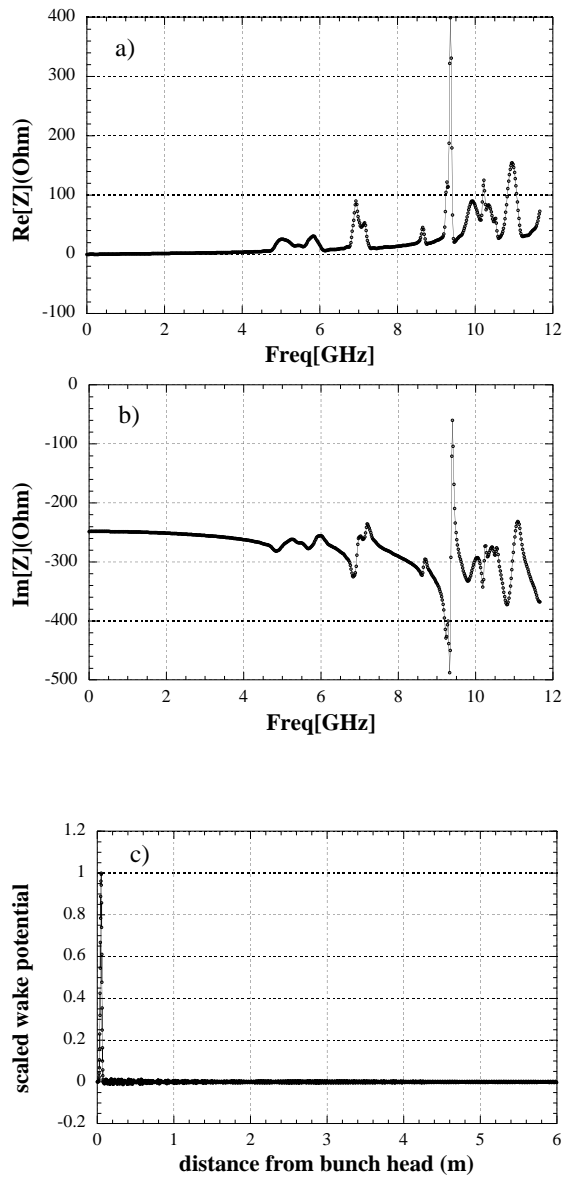


Figure 7: Transverse coupling impedance for  $N = 38$ : a) Real part, b) Imaginary part, c) Scaled wake potential.

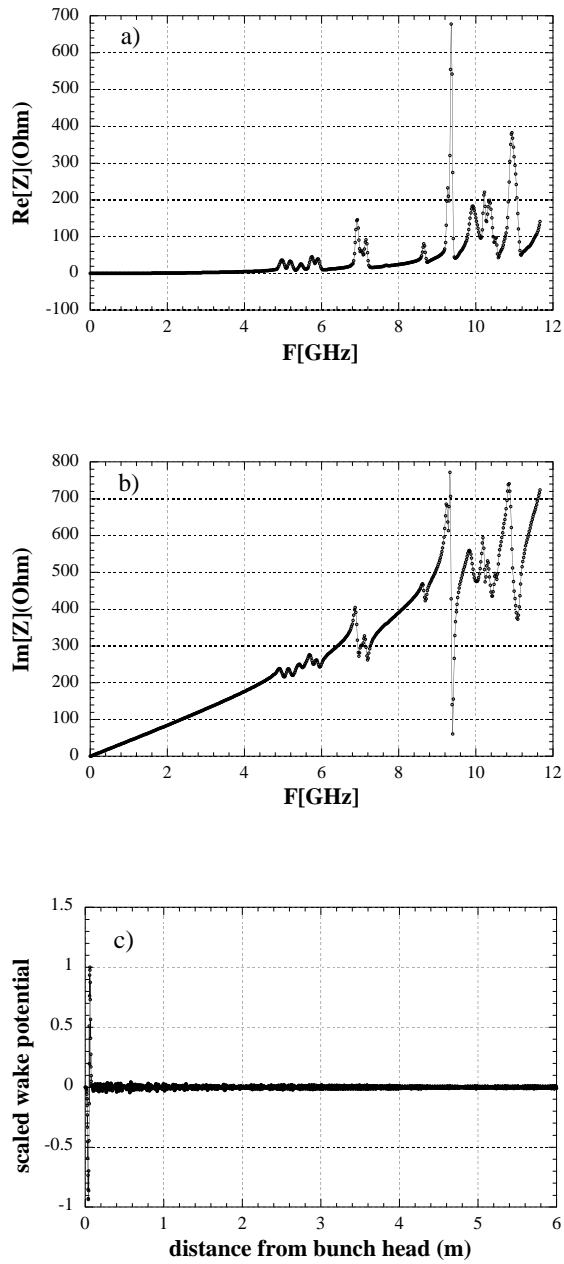


Figure 8: Longitudinal coupling impedance for  $N = 74$ : a) Real part, b) Imaginary part, c) Scaled wake potential.

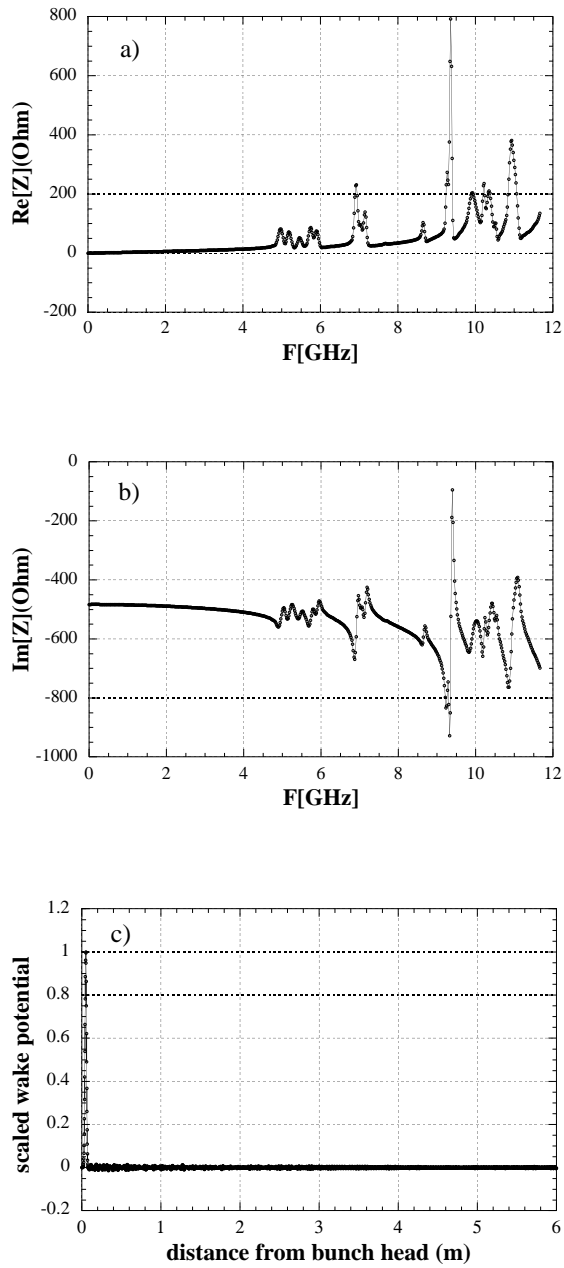


Figure 9: Transverse coupling impedance for  $N = 74$ : a) Real part, b) Imaginary part, c) Scaled wake potential.

coaxial outer short circuited with a length of  $l = 1.3$  m. The corresponding results are illustrated in Figs. 10a, 10b, 10c, and 11a, 11b, 11c.

As predictable, it is possible to observe a modulation of the impedance  $c/(2l) = 115$  MHz and higher quality factors of the parasitic modes because the resonant fields do not propagate in the coaxial line.

### 3.4 Whole beam screen with 146 holes (73 holes per row)

For the whole structure, a 4 mm longitudinal mesh was used due to limitation of the number of mesh points. Fig. 12a shows the longitudinal loss parameter and the power losses as a function of the horizontal displacement. It is clear that, for an off-set beam, the power losses increase considerably as it has been already discussed. As an example, a beam with  $x = 2.4$  cm off-set loses about  $P = 3.2$  mW that can affect machine operation.

To investigate the behavior of the power losses as a function of the beam pipe shape, different simulations were done changing the smaller axis of the elliptical beam pipe. Fig. 12b shows the power losses as function of the horizontal displacement for different values of the smaller axis  $a$ . The case with  $a = 33$  mm corresponds to the actual transition while that one with  $a = 42$  mm to a circular cross section.

We can observe that the circular shape gives less power losses than the actual one. This is an important element for the final section shape choice. We can observe that, in the elliptical cross section and in the center of the beam pipe, the power loss is  $P \sim 0.4$  mW (0.18 mW/m on overall transition) and the power gradient along the horizontal coordinate  $\partial P/\partial x = 0.054$  mW/mm with  $\partial K_l/\partial x = 1.65 \cdot 10^4$  V/(Cmm). Again, these values scale approximately as the square number of holes  $N^2$ .

Figure 12c shows the inductive behavior of the wake potential with  $\sigma = 12$  cm. The spikes observed are due to the large longitudinal mesh adopted for the present case. By assuming  $|W_{max}| = |W_{min}| = 7.3 \cdot 10^7$  V/C, we obtain  $|Z/n| = 13 \cdot 10^{-6}$   $\Omega$  which again scales as the hole number  $N$ . This result is also confirmed by the Fourier transform of the wake potential obtained with  $\sigma = 2$  cm over a distance of few meters behind the bunch which gives  $|Z/n| = 12 \cdot 10^{-6}$   $\Omega$  (Fig. 12d).

In Fig. 13 we show the transverse loss parameter as function of the transverse displacement. The horizontal impedance is  $Z_{tx} = 99$   $\Omega$ /m with  $\partial K_t/\partial x = 7 \cdot 10^{10}$  V/(Cm) while the vertical one is  $Z_{ty} = 30$   $\Omega$ /m with  $\partial K_t/\partial x = 2 \cdot 10^{10}$  V/(Cm). These values scale like the hole number  $N$ . A check of these results by using the Fourier transform of the wake potential gave 100  $\Omega$ /m and 29  $\Omega$ /m, respectively.

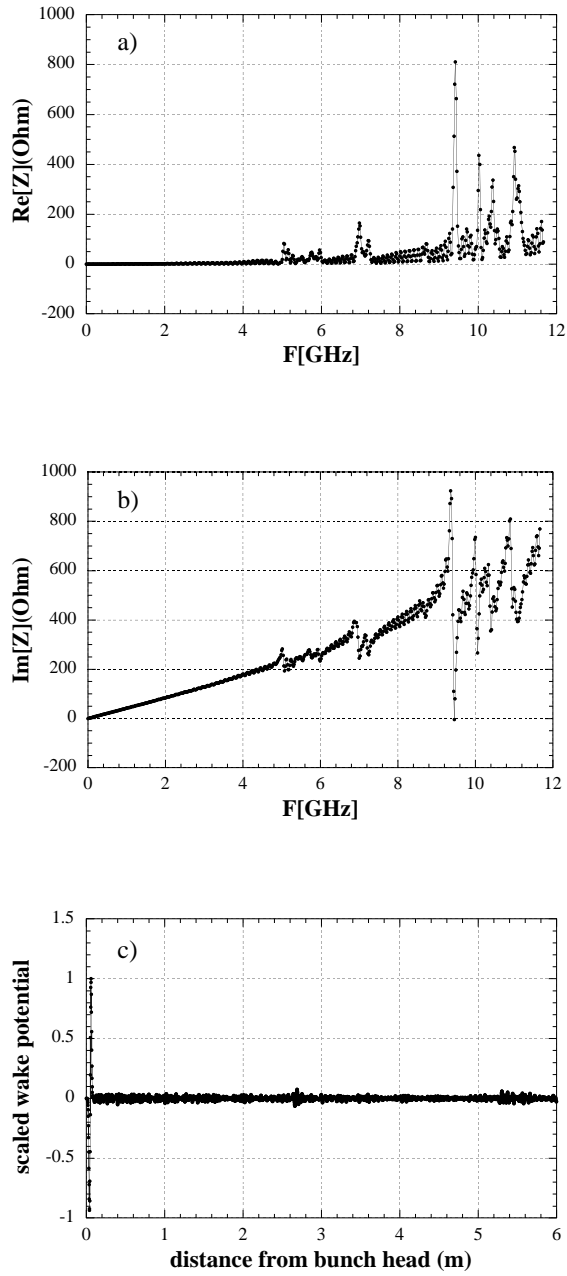


Figure 10: Longitudinal coupling impedance for  $N = 74$  with a coaxial length  $l = 1.3$  m:  
a) Real part, b) Imaginary part, c) Scaled wake potential.

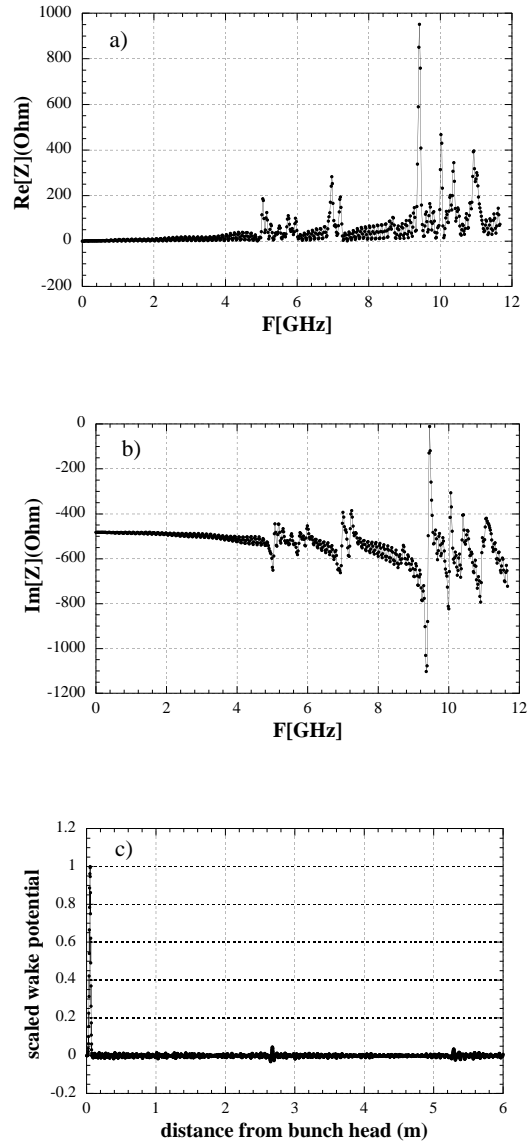


Figure 11: Transverse coupling impedance for  $N = 74$  with a coaxial length  $l = 1.3$  m: a) Real part, b) Imaginary part, c) Scaled wake potential.

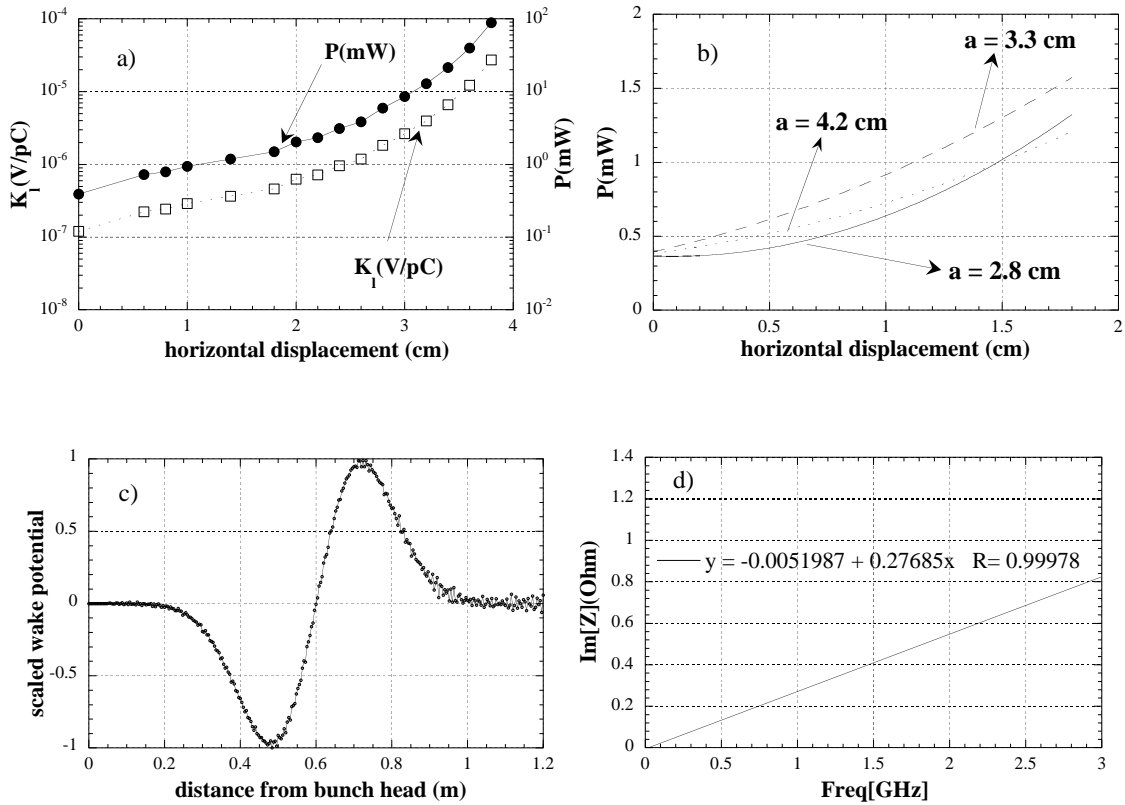


Figure 12: Whole cold transition with  $N = 146$ : a) Longitudinal loss parameter and power losses as a function of the horizontal displacement, b) Power losses as a function of the horizontal displacement for some values of the vertical axis by keeping unchanged the horizontal one, c) Wake potential normalized to its maximum value as a function of the distance from bunch head ( $W_{max} = 7.3 \cdot 10^7$  V/C), d) Fit of the imaginary part of the longitudinal broad band coupling impedance.

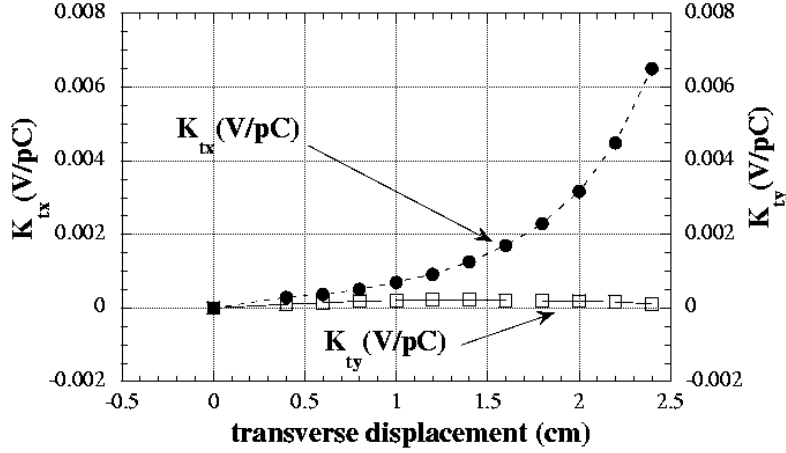


Figure 13: Horizontal and vertical loss parameter as a function of the transverse displacement for the whole cold transition with  $N = 146$ .

#### 4 Cold/Warm transition

The cold/warm transition is a tapered transition between the circular vacuum chamber and the elliptical one (Fig. 3). The analysis has been done separately for the input and output regions due to the limitation in the number of mesh points. The detailed study of the warm transition did not give specific problem and we will present only the final results.

The longitudinal impedance of the global structure is estimated to be  $|Z/n| = 0.31$   $m\Omega$ . The vertical transverse impedance is  $Z_{ty} = 707$   $\Omega/m$  while the horizontal one is  $Z_{tx} = 382$   $\Omega/m$ .

#### 5 Analytical estimations for the elliptical COLDEX beam screen and cold/warm transition

Even though in the present study the chamber has a beam pipe with elliptical cross-section, and therefore a correct approach to the solution of the problem needs three-dimensional codes, the analytical methods remain extremely useful to check the order of magnitude of the discussed numerical results.

We remark that the analytical model discussed above is valid for a coaxial beam pipe with axial symmetry, it neglects the effects due to the curvature of the chamber ( $a \ll b$  being  $a$  the hole radius and  $b$  the chamber radius), it assumes zero wall thickness of the

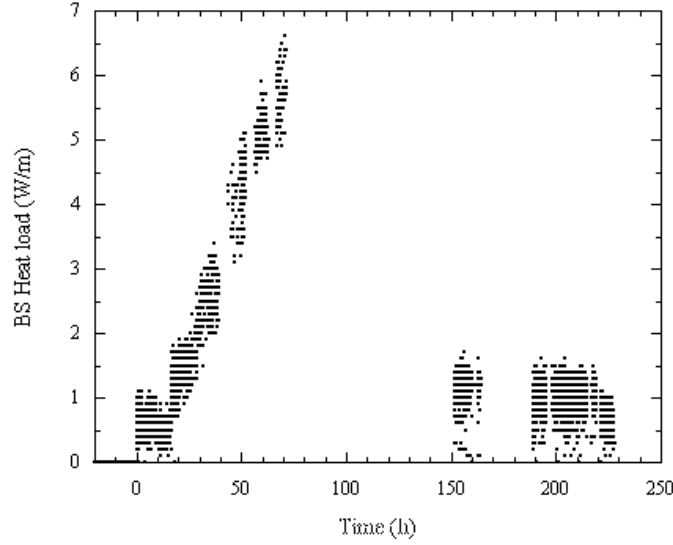


Figure 14: Heat load due to condensed gases onto the beam screen when two SPS batches were circulated through COLDEX [2].

circular hole and finally it considers the approximation of an incident plane wave (fields constant over the hole).

Nevertheless, for the longitudinal analysis, if we introduce an equivalent circular radius due to the ellipticity of the beam pipe [10]  $b_{eq}$ , and by taking into account the wall thickness correction factors on the polarizabilities [11], we can still apply the theoretical model.

As a result for the COLDEX beam screen with a number of holes  $N = 146$ , by assuming an equivalent chamber radius  $b = b_{eq} = 0.0374$  m and by keeping unchanged the outer one (Fig. 2), with a hole wall thickness of 2 mm, we get  $Z/n = 16.5 \mu\Omega$  and a power loss  $P = 0.43$  mW (eq. (7)). By assuming instead an internal radius equal to  $b = 0.043$  m, we obtain  $Z/n = 12.3 \mu\Omega$  and  $P = 0.55$  mW. The corresponding numerical estimations (about  $Z/n = 12 \mu\Omega$  and  $P = 0.4$  mW) are in good agreement with the previous ones. These values are given for a continuous train of bunches circulating in the SPS ring, which is not the case. In reality, the SPS is filled by 4 trains of batches of 72 bunches spaced by 25 ns. The batches are separated by gaps of 325 ns. In this case the average current has been estimated to be 58 mA per batch. The average power lost by the beam can be estimated with eq. (9) with  $N_b = 4$  (number of batches). The final contribution of the power losses to the COLDEX beam screen is therefore about 37 mW (that is 17 mW/m) on overall transition.

## 6 Conclusions

We presented the impedance study of the cold bore experiment, COLDEX, installed in 2002 in the SPS machine. The numerical estimations of the coupling impedance have been compared to a theoretical model showing a good agreement. Largely off-set beam deposits higher power. The most pessimistic case foresees an off-set of 10 mm, but during normal operation a maximum off-set of about 2 mm is expected [12]. The obtained ohmic losses are a few tens of mW. The losses in the cold/warm transition are negligible. Finally, in the unlikely case of a rapid cool down which could disconnect the cold/warm transition from the COLDEX beam screen by 5 mm for instance, the ohmic losses are still negligible. The sum of these losses is much less than the measured dissipated power in the COLDEX beam screen as shown in Fig. 14 [2].

In fact the first parasitic resonance is at about 5 GHz as it is shown for instance in Figs. 8a, b and 9a, b. If the bunch length is 12 cm, that corresponds to a cut-off frequency of 400 MHz, the effect of such impedance to the beam is surely negligible because the bunch spectrum lines are very far from the parasitic resonance itself.

Concerning the 5 mm discontinuity between the COLDEX beam screen and the cold/warm transition, we could expect (if the case) resonances with frequencies of the order of 60 GHz that are decoupled from the beam spectrum lines. Therefore we assume that there is no coupling between the beam with the beam screen and with the cold/warm transition as it confirmed by experimental tests.

This impedance study demonstrated that the heat load dissipated into COLDEX and due to the impedance seen by the beam is negligible as compared to the measured value. The observation of a dissipated power, a pressure rise and an electron activity inside COLDEX (all the effects appear above a given bunch current threshold) indicate the presence of an electron cloud [1,2,13]. So, the measured heat load in figure 14 is attributed to the presence of an electron cloud inside the COLDEX beam screen.

However the losses due to the pumping holes are of the order of few tens of mW. To fully simulate the LHC beam screen design with racetrack shape and pumping slots, it is therefore advisable to optimize the beam pipe shape. To this aim, in 2003, the COLDEX beam screen was a circular one of 67 mm diameter with two rows of 262 rounded slots (131 per row) spaced by 16.3 mm. Each slot is 2 mm wide and 7.5 mm long. The stainless steel cold/warm transitions of 0.1 mm thickness, were also improved. They are coated by 2  $\mu\text{m}$  of copper. Each extremity is bridged by radio frequency fingers. The middle of cold/warm transition is thermally anchored at 80 K. Finally the transition to the 100 mm diameter vacuum chamber is tapered with an angle of 45 degrees. All these precautions definitively ensure that the COLDEX experiment is protected against parasitic losses due

to impedance [13].

## References

- [1] V. Baglin, I.R. Collins, B. Jenninger, “Performance of a Cryogenic Vacuum System (COLDEX) with a LHC Type Beam”, *Vacuum* 73 (2004), pp. 201-206.
- [2] V. Baglin, B. Jenninger, “Gas Condensates onto a LHC Type Cryogenic Vacuum System Subjected to Electron Cloud”, CERN LHC Project Report 742, August 2004, presented at the 9th European Particle Accelerator Conference (EPAC’04) 5-9 July 2004, Lucerne, Switzerland.
- [3] R. Klatt et al., “MAFIA - a three dimensional electromagnetic CAD system for magnets, RF structures and transient wake-field calculations”, *Proceedings of the 1986 Linear Conference*, Stanford Linear Accelerator Center, SLAC-Report 303, June 1986 (pp. 276-278).
- [4] A. Mostacci, L. Palumbo and F. Ruggiero, “ Impedance and loss factor of a coaxial liner with many holes: effect of the attenuation”, *Phys. Rev. ST-AB*, **2**, 124401, 1999.
- [5] A. Mostacci, “Energy lost by a particle beam in a lossy coaxial liner with many holes”, LHC Project Report 199, February 2002.
- [6] L. Palumbo, V. G. Vaccaro, M. Zobov, “Wake Fields and Impedance”, LNF-94/041 (P), September 1994.
- [7] G. V. Stupakov, “Geometrical wake of a smooth taper”, SLAC-PUB-95-7086, Dec. 1995.
- [8] B. Spataro et al., “Broad-band model impedance for DAΦNE main rings”, *NIM A* (1994) 231-241.
- [9] P. Fernandes and R. Parodi, *IEEE Trans. on Magn.*, 21(6) (1985) p. 2246.
- [10] L. Palumbo, et al., “Coupling Impedance in a Circular Particle Accelerator, a Particular Case: Circular Beam, Elliptical Chamber”, *IEEE Trans. on Nuclear Science*, Vol. NS-31, n. 4, August 1984.
- [11] Noel A. McDonald, “Electric and Magnetic Coupling Impedance through Small Apertures in Shield Walls of Any Thickness”, *IEEE Trans. on microwave and techniques*, Vol. MTT-20, n. 10, 1972.

[12] G. Arduini, private communication.

[13] V. Baglin, B. Jenninger, "Pressure and Heat Load in a LHC Type Cryogenic Vacuum Chamber System Subjected to Electron Cloud", CERN LHC Project Report 721, July 2004, presented at the 31st ICFA Advanced Beam Dynamics Workshop on Electron-Cloud Effects (E-CLOUD'04) 19-23 April 2004, Napa (California), USA.